Ignition Delay and Combustion Characteristics of Gaseous Fuel Jets

Dung Ngoc Nguyen[1]
e-mail: dungnn2@elan.energy.kyoto-u.ac.jp

Hiroaki Ishida

Masahiro Shioji

Graduate School of Energy Science,
Kyoto University,
Yoshida-Honmachi, Sakyo-ku,
Kyoto 606-8501, Japan

Gaseous fuels, such as hydrogen and natural gas, are utilized in internal combustion engines for spark-ignition operation. To improve thermal efficiency and to ensure control at good heat-release rates, combustion systems with direct-injection and spontaneous-ignition operation may be preferable. The main objective of this research was to provide fundamental data for the ignition and combustion of hydrogen, natural gas, and methane. Experiments were conducted in a constant-volume combustion vessel to investigate the effects of ambient temperature on ignition delay and combustion characteristics for various injector and ambient conditions. Experimental results showed that all gaseous fuels exhibited similar ignition-delay trends: ignition delay (τ) increased as ambient temperature (T_i) decreased. Among these fuels, hydrogen jets exhibited much shorter τ than natural gas and methane jets at the same T_i and could be ignited at a lower temperature, $T_i = 780$ K. A shorter ignition delay of hydrogen may be attained by controlling the mixture formation by lowering the injection pressure (p_j), enlarging the nozzle-hole diameter (d_N), increasing the ambient pressure (p_i), and increasing the oxygen mole fraction (r_{O2}). In contrast, the methane jet exhibited the longest τ over the whole range of T_i and suffered from misfiring at a higher T_i of 910 K. For natural gas, ignition delay was observed to be shorter than that for methane, owing to a small amount of butane with good ignitability. More specifically, the ignition delay of natural gas differed slightly when d_N and p_j varied but changed drastically when p_i and r_{O2} decreased. Based on these data, the feasibility of gaseous fuels for compression-ignition engines is discussed from the viewpoint of mixture formation and chemical reaction.
[DOI: 10.1115/1.4000115]

Keywords: ignition delay, combustion characteristics, gaseous fuel jets, hydrogen, natural gas, methane

1 Introduction

The use of fossil fuels as the main energy source for internal combustion engines has changed people's lives more than any other invention. These fuels have played a crucial role in economic development. However, the use of fossil fuels has resulted in the emission of serious pollutants that are destroying the environment and harming people's lives. With the increase in concern surrounding energy security and environmental issues, many alternative fuels, including gaseous and liquid forms, have been introduced and applied to internal combustion engines. Among these, hydrogen and natural gas are considered to be some of the most promising fuels, since they can replace conventional petroleum and reduce tailpipe emissions. Hydrogen can be produced entirely from water and can meet ever-stringent regulations concerning the future emission of greenhouse and exhaust gas. In addition, natural gas is a vital component of the world's energy supply, as well as one of the cleanest burning alternative fuels and is produced abundantly from natural resources all over the world.

Researchers have been interested in applying hydrogen as a fuel for internal combustion engines over many decades [1–9]. Hydrogen has unique properties as a fuel and is more advantageous than other alternative fuels. These advantages include minimum emissions of hydrocarbons, carbon dioxide, smoke [10], and greatly improved cold-start capability. Hydrogen fuel jets exhibit desirable characteristics for spark-ignition engines. This gaseous fuel has broad flammability limits, high flame propagation, high burning velocity, low ignition energy, and high autoignition temperature over a wide range of temperatures and pressures. With this broad flammability range, hydrogen engines can easily combust and produce energy over a wide range of fuel-air mixtures; thus, hydrogen engines could operate with a very lean equivalence ratio. Lean-mixture operation in combination with fast combustion near top dead center (TDC) results in a short combustion period, high thermal efficiency output, and low NO_x levels [11]. The low ignition energy could reduce cyclic variation for hydrogen engines even for very-lean-mixture operation. This leads to reduction in emissions, improvement in thermal efficiency, and smoother engine operation [12]. Furthermore, the fast-burning characteristics satisfy the requirements of hydrogen engines regarding high-speed engine operation. This may permit increased direct power output for lean-mixture operation [13,14]. These unique features have attracted many researchers to create high-efficiency hydrogen engines [15,16].

However, there are many reports concerning the performance problems of hydrogen engines. Engines fueled with hydrogen are subject to reduced power output owing to the low heating value of hydrogen in basic volume and lean-mixture operation [12]. The low ignition energy causes problems, such as premature ignition and flashback, as a result of its autoignition by hot gases and hot spots in the combustion chamber. The smaller quenching distance may increase the tendency to backfire since the flame from a hydrogen-air mixture more readily passes a nearly closed intake valve [8,11,17,18]. In addition, the high burning rate of hydrogen produces high-pressure and high temperature during combustion,

[1]Corresponding author.

Contributed by the IC Engine Division of ASME for publication in the JOURNAL OF ENGINEERING FOR GAS TURBINES AND POWER. Manuscript received April 8, 2009; final manuscript revised July 24, 2009; published online January 27, 2010. Assoc. Editor: Kalyan Annamalai.

which leads to knock, high exhaust-gas emissions of NO_x, and increases in engine vibration and noise. Many methods have been proposed to overcome these problems. These include decreasing the temperature of the ignition sources, optimizing injection and spark timing, using lean-burn techniques, reducing crevice volume, and eliminating abnormal discharges. However, these techniques have not been successful in controlling backfire and engine performance. Recently, internal mixing of hydrogen achieved by high-pressure injection systems has been introduced and applied to prevent backfire and knock, particularly under high-load operation [5,16,19–21].

Natural gas is a type of fossil fuel and is a promising substitute for petroleum. Natural gas has been widely used in homogeneous-charge spark-ignition engines for cogeneration systems, heat pumps, and vehicles. Natural-gas engines are advantageous in terms of the emission of fewer smoke pollutants and fewer greenhouse gases [22–25] compared with conventional petroleum. Conventional natural-gas engines are limited in power and thermal efficiency relative to diesel engines owing to knock under high-load, and they need to operate at stoichiometric fuel/air ratio conditions together with three-way catalysts to achieve emissions reduction [26]. In order to attain higher thermal efficiency in natural-gas engines and to overcome abnormal-combustion problems, direct-injection and spontaneous-ignition operations may be preferable. Recently, glow-plug assisted direct-injection natural-gas engines have been used in an attempt to attain higher thermal efficiency [27]. However, control over mixing is still the main obstacle for this application, particularly under low-load operation.

Direct-injection technology has been developed and applied to both hydrogen and natural-gas engines in an effort to reduce the effects of abnormal combustion. This method is very effective in increasing combustion efficiency and engine power and in obtaining cleaner emissions in an onboard engine. Previous studies have successfully applied direct-injection of hydrogen and natural gas to both spark-ignition and compression-ignition engines [28,29]. However, the ignition and combustion of transient and high-pressure gaseous jets are not well understood at present [20,30,31]. To increase thermal efficiency and to benefit from potential reductions in exhaust-gas emissions, the utilization of direct-injection combustion by the optimum control of ignition and mixing is needed.

Continuing with our previous research on the spark-ignition and combustion characteristics of high-pressure hydrogen injection and intermittent natural-gas jets [21], the main objective of the present research was to obtain fundamental data regarding the ignition delay and combustion characteristics of hydrogen, natural gas, and methane jets under direct-injection compression-ignition conditions. Experimental ignition delay and combustion characteristics were tested in a constant-volume combustion vessel under a variety of conditions, including ambient temperature (T_i), nozzle-hole diameter (d_N), injection pressure (p_j), ambient pressure (p_i), and oxygen concentration (r_{O2}). In particular, based on the obtained results, the mechanism of ignition and combustion in gaseous fuel jets is discussed with emphasis on mixture formation.

2 Experimental Setup and Procedure

In our present research, experiments on ignition delay and combustion characteristics for spontaneous gas jets were conducted using a constant-volume combustion vessel. Figure 1 shows a schematic of the cross section of the combustion chamber. The chamber is a circular cylinder, 80 mm in diameter, 30 mm in depth, approximately 150 cm^3 in volume, and fitted with quartz windows in both sizes for allowing full optical assessment. A high-pressure solenoid-type single-shot gas injector, fitted at the top of the chamber, was used to inject gaseous fuel into the combustion chamber. This special injector could inject gaseous fuels to a maximum of 15 MPa. Fuel quantity and equivalence ratio of the mixture were controlled by adjusting the injection duration.

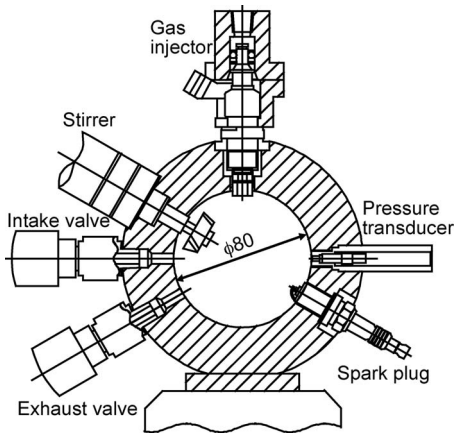

Fig. 1 Cross section of constant-volume combustion vessel

An intake valve was used to charge and adjust the initial premixed gas in the chamber, while an exhaust valve was used to remove burned gas. A mixing fan (or stirrer) was used to maintain a uniform temperature in the chamber before fuel injection; stirrer speed was then kept constant. Pressure in the combustion chamber was measured using a piezoelectric absolute-pressure transducer (Kistler 6052A). The obtained pressure was used to determine ignition delay and to calculate the heat-release rate. The definition of ignition delay for hydrogen and natural-gas jets corresponds to that in Ref. [5]. In the current paper, ignition delay is defined as the time from the start of injection until the net rate of pressure-rise exceeds the employed threshold level of 50 MPa/s. Reacting jets and flame penetration were visually investigated with a high-speed shadowgraph using a complementary metal oxide semiconductor (CMOS) digital camera (Vision Research, Phantom V7.0). To reduce the effect of vapor on the combustion windows and to obtain high-quality shadowgraph photos, these windows were heated to 230°C before every experiment. In this study, photographs were captured at a speed of 10,000 fps and an exposure duration of 30 μs.

The two-step combustion discussed in Ref. [31] was used to simulate diesel TDC combustion processes in the constant-volume combustion vessel. To start the experiment, premixed gas (C_2H_4, H_2, O_2, and N_2) prepared in a mixing tank was introduced into the combustion chamber through the intake valve and ignited by a spark plug. The initial pressure of premixed combustible gas was selected so that the temperature, pressure, and oxygen mole fraction corresponded with diesel combustion near TDC. The vessel temperature was determined as a thermodynamically averaged temperature via a known initial temperature, initial pressure, and composition of the premixed gas before ignition [20]. After the combustion of the premixed charge, the pressure decayed as a result of heat transfer to the walls. When the desired temperature and pressure were obtained, a signal was transmitted to actuate the gas injector. Injection fuel then autoignited and burnt in an appropriate environment. To eliminate large-scale temperature distribution in the combustion chamber and to ensure homogeneous conditions before injection, a mixing fan was run 20 s before the ignition of the premixed combustible gas.

Table 1 shows the experimental conditions for the present study. Three gaseous fuels, hydrogen, natural gas (CH_4 88%, C_2H_6 6%, C_3H_8 4%, and C_4H_{10} 2%), and methane, were studied. The underlined numbers in the table correspond to the base conditions. Fuel quantity was selected so as to obtain an equivalence ratio ϕ=0.33 at the base condition of T_i=1000 K for each fuel, and the injection duration was fixed irrespective of ambient temperature. The effects of injector parameters on ignition and combustion were studied by varying the nozzle-hole diameter d_N =0.56, 0.8, and 1.1 mm and injection pressure p_j=6, 8, and 10

Table 1 Experimental conditions

Fuel		H_2, NG	CH_4
Injection pressure, p_j	MPa	6, 8, 10	8
Ambient pressure, p_i	MPa	2, 3, 4, 5	4
Ambient temperature, T_i	K	700–1200	700–1200
Nozzle-hole diameter, d_N	mm	0.56, 0.8, 1.1	0.8
Oxygen concentration, r_{O2}	%	21,15, 10	21

MPa; the effects of combustion environments were investigated by varying ambient pressure p_i=3, 4, and 5 MPa and reducing oxygen concentrations from 21% to 10%. For each test parameter, the ambient temperature (T_i) was varied in the range of 700–1200 K so as to observe its effects on ignition and combustion.

3 Combustion Analysis

Combustion characteristics of the tested fuels were analyzed and compared using the heat-release rate dq/dt calculated via the obtained pressure history. Essentially, the heat-release rate is the heat value generated per unit of time by combustion. The value of dq/dt depends on ignition delay, the properties of the fuel, and injection and combustion conditions. The method for calculating dq/dt for a constant-volume combustion vessel is described as follows.

An energy equation with enthalpy balance due to heat transfer and fuel injection is expressed by the following equation:

$$-dQ_c = dH + dH_f - Vdp \tag{1}$$

where dQ_c is the enthalpy variation by heat transfer, dH is the total enthalpy of operating gases inside the combustion vessel, dH_f is the enthalpy balance by fuel injection, V is the combustion vessel volume, and p is the pressure inside the chamber.

The total enthalpy, including sensible enthalpy and enthalpy of formation, is expressed as follows:

$$dH = d\left[\sum_i n_i\left\{h_{fi}^{T_0} + \int_{T_0}^{T} C_{pi}(\beta)d\beta\right\}\right] = \sum_i h_{fi}^{T_0} dn_i + \sum_i \left\{\int_{T_0}^{T} C_{pi}(\beta)d\beta\right\}\cdot dn_i + \sum_i n_i C_{pi}(T)dT \tag{2}$$

where n_i is the mole number of species i, $h_{fi}{}^{T0}$ is the enthalpy of formation of species i at standard temperature T_0, and C_{pi} is the specific heat at constant pressure of the component i.

The third part to the right of Eq. (2) is the variation of sensible enthalpy due to temperature. The second part is sensible enthalpy change caused by alteration of dn_i and chemical reaction. The first part is enthalpy of formation, which is changed by chemical reaction, and is known as heat quantity release by combustion. The first part is replaced by dQ_B. If enthalpy of formation is negative, dQ_B is positive. The gases are regarded as ideal gases. By substituting Eq. (2) into Eq. (1) and differentiating over time, the following equations are derived and used to calculate the rate of heat release:

$$\frac{dQ_B}{dt} = \frac{dQ_c}{dt} + \left\{\frac{\bar{C}_p(T)}{R} - 1\right\}\cdot V\frac{dp}{dt} + \sum_i \{h_i(T) - h_i(T_0)\}\cdot\frac{dn_i}{dt} + \sum_j h_j(T_F)\frac{dn_{Fj}}{dt} \tag{3}$$

where R is the universal gas constant, T_f is the fuel temperature, dn_{Fj}/dt is the injection rate (mol/s) of species j in fuel, $\bar{C}_p = \Sigma_i n_i C_{pi}(T)/\Sigma_i n_i$ is the mean specific heat, and $h_i(T) = h_{fi}^{T_0} + \int_{T_0}^{T} C_{pi}(\beta)d\beta$ is the total enthalpy derived from Prothero's equation.

Fuel is assumed to burn completely. The mole rate of burned fuel dn_i/dt is calculated by dividing (dQ_B/dt) by low calorific value. In this research, the low calorific values of hydrogen, natural gas, and methane are 120.95 MJ/kg, 43.94 MJ/kg, and 50.17 MJ/kg, respectively. Once dn_i/dt has been calculated, the total mole number can then be calculated, and temperature T in the chamber can be determined using the state equation of an ideal gas.

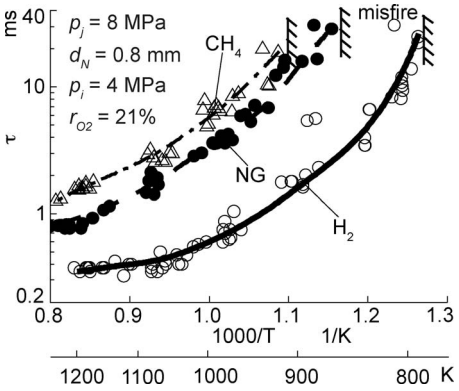

Fig. 2 Effects of T_i on t for H_2, NG, and CH_4

4 Results and Discussions

The results and discussions are presented in five parts. In Sec. 4.1, we focus on analyzing the effect of ambient temperature T_i on ignition and combustion for hydrogen, natural gas, and methane jets. Ignition delay is plotted in Arrhenius forms, reflecting the importance of chemical kinetics, and Arrhenius lines are then defined as basic ignition lines. Sections 4.2 and 4.3 discuss the effects of nozzle-hole diameter and injection pressure on ignition and combustion. Section 4.4 concerns the effects of ambient pressure. Finally, we discuss the effects of oxygen concentration.

4.1 Ignition and Combustion Characteristics at the Base Condition for Various Gaseous Fuel Jets. In diesel-combustion conditions, studies of various liquid sprays found that the ambient temperature had a large effect on ignition delay. This dependence is associated with mixture formation and chemical kinetics during the autoignition period of fuels. In this part, we focus on discussing the effects of ambient temperature on the ignition delay and combustion characteristics for hydrogen, natural gas, and methane jets at the base condition.

Figure 2 shows the effect of ambient temperature on τ for each gaseous fuel jet in Arrhenius form. Each gaseous fuel jet exhibits a corresponding τ trend. As T_i decreases, the ignition delay increases slightly at higher T_i but greatly at lower T_i. Among the tested fuels, the hydrogen jet presents the shortest τ for the same T_i and could be ignited at the lowest T_i (780 K). In contrast, the methane jet shows the longest τ over the whole range of T_i and suffers from misfiring at a higher T_i of 910 K. The natural-gas jet has shorter τ than that of the methane jet owing to a small amount of butane with good ignitability. Ignition-delay values of the hydrogen jet can be seen to be greatly scattered at temperatures lower than 900 K, which may be attributed to the ignition mechanism of the hydrogen fuel jet with a chain carrier sensitive reactions.

From these obtained results, a short ignition delay of 1–2 ms for use in compression-ignition engines can be obtained at ambient temperatures above 1100 K for methane and natural gas and above 900 K for hydrogen jets. For methane and natural-gas jets, this temperature is much higher than TDC compression temperatures in direct-injection diesel engines, typically around 800 K, which

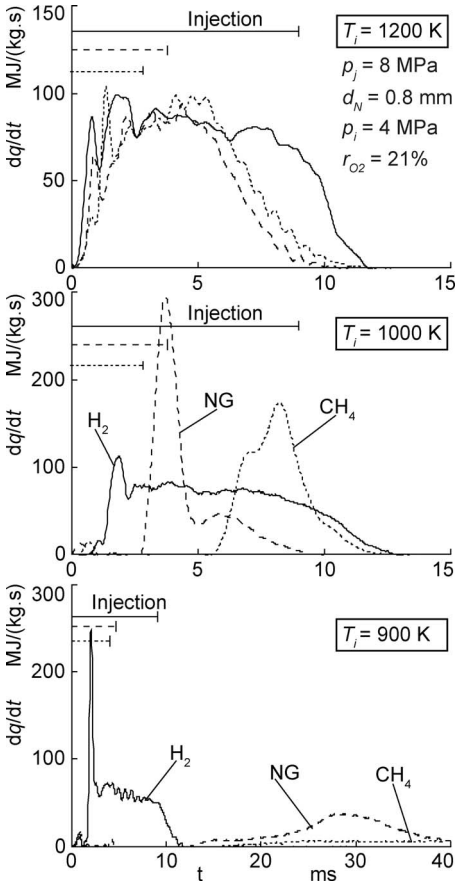

Fig. 3 Effects of T_i on dq/dt for H_2, NG, and CH_4

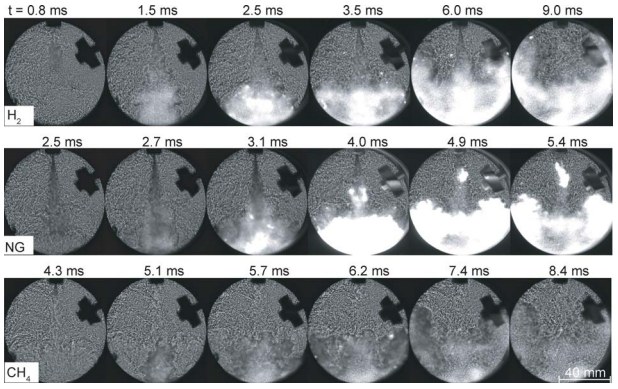

Fig. 4 Shadowgraph images of jet and flame developments for H_2, NG, and CH_4 at T_i=1000 K

implies that some countermeasures are necessary to assist the ignition. On the other hand, for hydrogen jets the temperature for a reasonable delay is slightly higher under diesel-engine conditions, suggesting the potential for realizing a direct-injection compression-ignition engine.

The combustion processes of these gaseous fuel jets are shown in Fig. 3, with the results of dq/dt at three different temperatures. At T_i=1200 K, the typical progress of dq/dt is demonstrated for all fuels: premixed combustion occurs after τ, followed by diffusive combustion with a lower and constant dq/dt. The hydrogen jet exhibits a corresponding trend in dq/dt curves at different T_i under variations in τ. Natural gas and methane jets, however, exhibit a drastic change in dq/dt curves. The injection fuels are mixed well with air during long τ, and then only premixed combustion is observed at T_i=1000 K. At a lower T_i of 900 K, below the misfire limit of methane, the reaction rate of natural gas is greatly decreased, resulting in a very low dq/dt. The results of dq/dt at three different values of T_i confirm the previous discussion concerning an appropriately short τ for suitable use in compression-ignition engines. The hydrogen jet exhibits dq/dt comparable to natural gas and methane at T_i=1200 K and possibly autoignites during injection at the tested T_i. The dq/dt curves of natural gas and methane jets are observed to differ greatly at T_i, which reflects the differing combustion characteristics for natural gas and methane due to a τ that is excessively long and a low chemical reaction rate.

The combustion processes are explained in more detail via the development of fuel jets and flames. Figure 4 shows the shadowgraph images observed at T_i=1000 K for each fuel, and the time of injection (t) is indicated on the individual image. The first photograph in each line for each fuel shows the jet development just before ignition, and the later photographs demonstrate the combustion progress in the flaming region. For hydrogen fuel, spontaneous-ignition occurred within 1 ms after injection, and the flame then spread downstream of the jet until 1.5 ms. Subsequently, diffusion combustion proceeded as the injection fuel penetrated the hot zone. Consequently, the flaming region expanded immediately followed by jet development. In contrast, in the cases of natural gas and methane, the mixture accumulated during the longer τ and burned quickly, resulting in the rapid expansion of the flaming region from the vicinity of the chamber wall to the center.

4.2 Effects of Varying Nozzle-Hole Diameters. Nozzle-hole diameter (d_N) is one of the most significant and fundamental parameters in designing combustion systems for direct-injection compression-ignition engines. A single-shot gas injector was used in this study, and d_N was changed to 0.56 mm, 0.8 mm, and 1.1 mm at a fixed gas source pressure of 8 MPa. The effects of nozzle-hole diameters on ignition and combustion for hydrogen and natural-gas jets are discussed based on the experimental data of τ and dq/dt with the variation in T_i shown in Figs. 5 and 6.

Figure 5 shows the effects of d_N on τ for hydrogen and natural-gas jets. For hydrogen jets, a larger d_N gives shorter τ at low T_i, and the difference in τ among d_N becomes smaller at higher T_i. For natural-gas jets, τ exhibits contrasting trends at T_i higher and lower than 1000 K. At a lower temperature, autoignition occurred after injection ended for every d_N, and the ignition trend for larger d_N is smaller in this figure. However, this trend exhibits contrasting results for a higher T_i, owing to greater chemical mixing and a higher reaction rate. Natural-gas jets autoignited during the injection period, and a shorter τ end is observed with smaller d_N.

The above discussions for natural-gas jets suggest that the τ of natural gas is controlled by mixture formation with different d_N. Under the condition of lower T_i with a larger τ, the jet with a small d_N formed an excessively lean-mixture during long τ, resulting in a very slow reaction. At a higher T_i, the reaction started at a point that satisfied the ignition condition, and τ then became shorter with faster mixture formation for a smaller d_N. On the

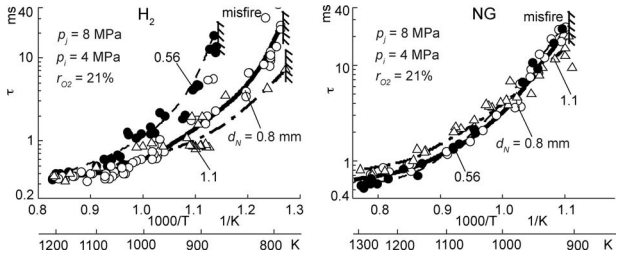

Fig. 5 Effects of d_N on τ for H_2 and NG jets

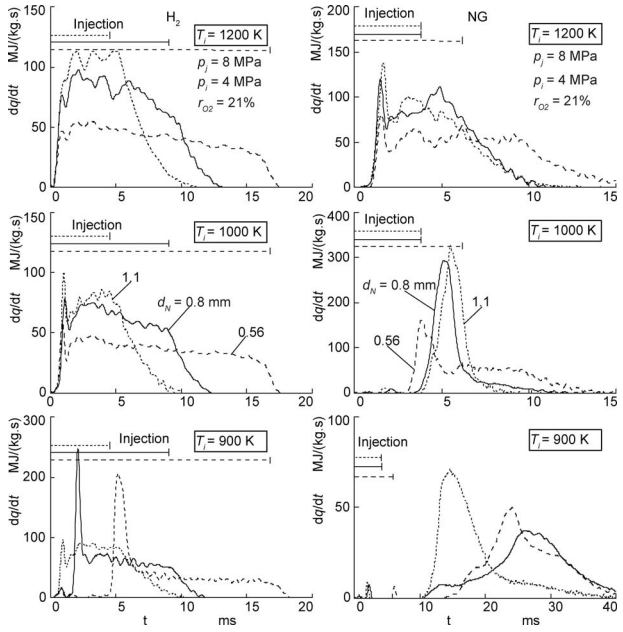

Fig. 6 Effects of d_N on dq/dt for H_2 and NG jets

other hand, in the case of different hydrogen jets, with high flammability, the injected hydrogen immediately mixed with burned premixture gas and autoignited just after injecting time. Thus, the ignition delay tends to be shorter as the amount of injection fuel is larger. At the same gas source pressure of 8 MPa, a larger d_N produced a higher injection rate, and a large amount of hydrogen fuel was thus injected over time, with high rate of chemical reaction and fast mixing promoting shorter τ with larger d_N.

Figure 6 shows the change in dq/dt curves with the change in d_N for both hydrogen and natural-gas jets at different T_i. Injection duration for each gas jet is also indicated in the figure. With the variation in d_N and T_i, hydrogen combustion exhibits corresponding dq/dt curves, while the results of natural gas change drastically with the variation in T_i. The relationship between mixture formation and τ is reflected in the following combustion processes. At T_i=1000 K, the initial peak in dq/dt increases with an increase in d_N. In every case for hydrogen jets, ignition occurred within the injection period. A larger d_N with higher injection rate displayed a higher rate of initial combustion, and a constant dq/dt then continued until injection ended. The fast mixing and fast combustion processes for larger d_N are indicated by the higher dq/dt. In contrast, at a lower T_i for natural-gas jets, ignition occurred after injection ended, and only premixed combustion with a higher dq/dt was observed.

In real diesel combustion, change in d_N resulted in a minor effect on the ignition. Ignition delay was typically influenced by the parameters relative to chemical kinetics. The results in Fig. 5 show an opposite tendency in diesel-spray ignition with change across entire temperature range for hydrogen. The change in d_N had a large effect on τ owing to the high flammability and fast combustion characteristics of hydrogen jets. However, the combustion processes of hydrogen were not greatly affected by the change in T_i and d_N with corresponding dq/dt curves in Fig. 6. For natural-gas jets, nozzle-hole diameters did not greatly influence ignition, and the ignition trend corresponded with that for diesel sprays.

4.3 Effects of Varying Injection Pressures. Injection pressure (p_j) is another parameter pertaining to the combustion system of compression-ignition engines. For liquid sprays, a high injection pressure resulted in good atomization, smaller droplets, and good vaporization. On the other hand, for gaseous fuel jets, the

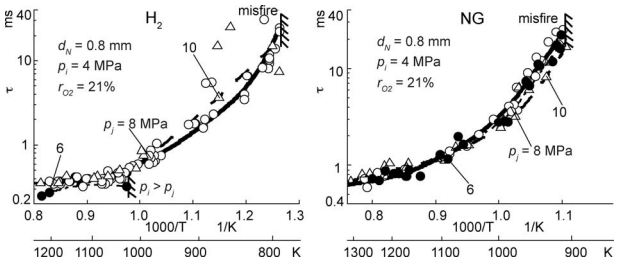

Fig. 7 Effects of p_j on τ for H_2 and NG jets

injected gas immediately mixed with surrounding air, and a mixture was formed. High injection pressure increased the injection rate and thus possibly affected the mixing process. In this research, hydrogen and natural gas were injected via a fixed d_N =0.8 mm while modifying p_j from 6 MPa to 10 MPa. In order to protect the injector, the experiment was stopped if the combustion chamber pressure was detected to be higher than the injector pressure ($p_i > p_j$) during the injection period. The experimental results of ignition delay and HRR with changing p_j and T_i are shown in Figs. 7 and 8

For hydrogen jets, the results in Fig. 7 show that a lower p_j gives shorter ignition delay. At $T_i > 1000$ K, the autoignition process for each p_j occurs during injection, and the shortest τ result is observed with p_j=6 MPa. At lower temperature, τ with p_j =10 MPa tends to be longer than that with p_j=8 MPa. The resulting short τ for the lower injection pressure of hydrogen jets suggests a different mixing process of hydrogen compared with other fuels. At lower injection pressure, the hydrogen jet easily dilutes across a wide area inside the chamber. Hydrogen-air mixture is formed over a wide region and, thus, tends to be autoignited faster. On the other hand, for higher p_j, a high injection rate results in increased mass flow rate for hydrogen jets. With this increase in rate, hydrogen jets penetrate and develop immediately following injector axial. Less hydrogen dilution reduces the mixing areas. In this case, mixing occurs only in the shear layer of the jet. Because of longer τ, as shown in Fig. 8, a higher injection pressure with a high injection rate exhibits higher dq/dt in initial combustion, and the injected fuel burns continuously at a constant

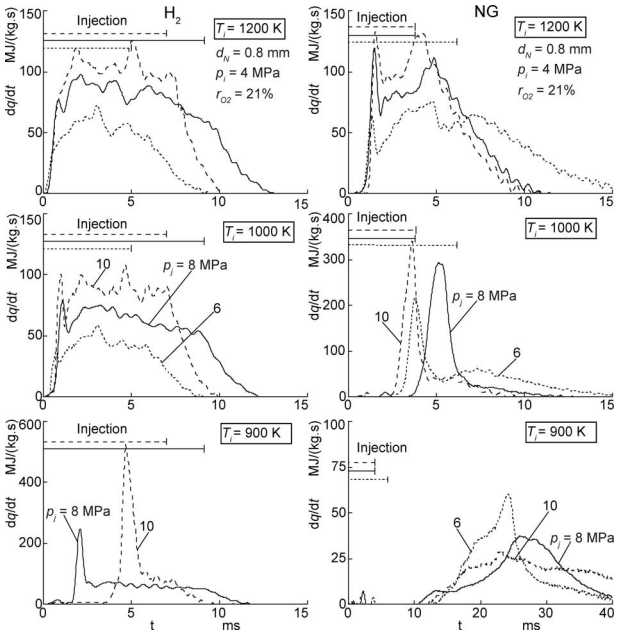

Fig. 8 Effects of p_j on dq/dt for H_2 and NG jets

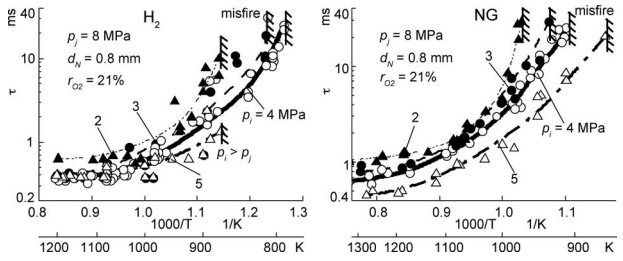

Fig. 9 Effects of p_i on τ for H_2 and NG jets

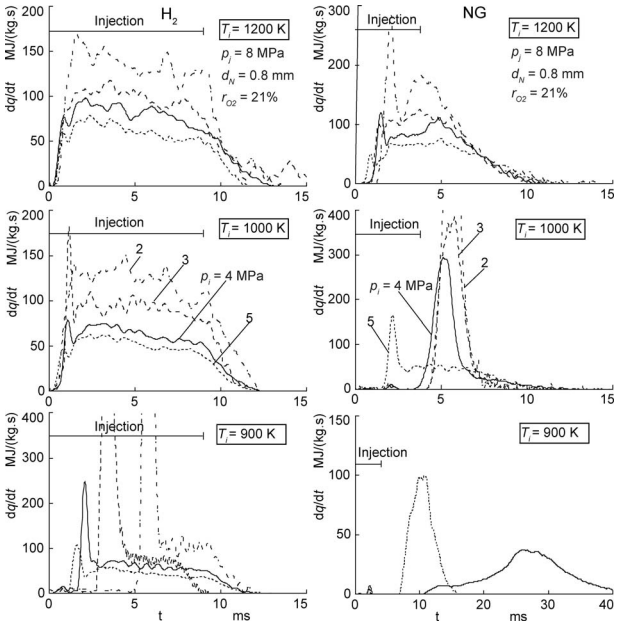

Fig. 10 Effects of p_i on dq/dt for H_2 and NG jets

rate of dq/dt until injection ends.

For natural-gas jets, the ignition-delay trend seems to differ from the result of hydrogen jets. Ignition delay with $p_j=6$ MPa and $p_j=8$ MPa is almost the same over the entire temperature range and mostly depends on temperature. In particular, for the result with $p_j=10$ MPa, the ignition-delay trend differs from that with standard $p_j=8$ MPa at high and low temperature. With T_i above 1050 K, the ignition-delay trend is observed to be longest with $p_j=10$ MPa. However, with T_i under 1000 K, the experimental results indicate the opposite trend. The ignition-delay trend with $p_j=10$ MPa corresponds with the result in the previous discussion with $d_N=1.1$ mm because both parameters cause an increase in the injection rate. Furthermore, in Fig. 8, high heat-release rate curves are also observed with higher injection pressure. Combustion histories of natural gas with representative dq/dt curves are similar for different injection pressures at known ambient temperature.

Several trends are summarized from the effects of injection conditions of d_N and p_j on the ignition delay and combustion characteristics for hydrogen and natural-gas jets. First, a suitably short τ for use in compression-ignition engines is above 900 K for hydrogen jets and over 1100 K for natural-gas jets. Second, at higher T_i, the τ values of hydrogen and natural gas are almost the same for different d_N and p_j owing to the high chemical reaction rate. However, τ trends differ for the results of these gaseous fuels. Third, ignition delay and dq/dt of hydrogen jets correspond well with the injection rate and the mixing region. For natural-gas jets, ignition delay with different d_N and p_j show different trends with temperature change. However, this change was small in comparison with hydrogen jets.

4.4 Effects of Varying Ambient Pressure. Ambient pressure and ambient temperature strongly affect the ignition and combustion of liquid sprays. Effects of T_i on ignition and combustion for hydrogen, natural gas, and methane were tested, as described in Sec. 1. In this section, we focus on the effect of p_i on τ and combustion characteristics. Experiments were carried out at $p_j=8$ MPa, $d_N=0.8$ mm, and $r_{O2}=21\%$ with variation in p_i from 2 MPa to 5 MPa. The change in p_i is appropriate for a large-engine operation range, from low to high-load. Similar to the variation of p_j, the experiment was stopped if we detected $p_i>p_j$ during injection to prevent damage to the injector.

The effects of p_i on τ for hydrogen and natural-gas jets are shown in the Arrhenius form in Fig. 9. According to this figure, the ignition-delay trend of hydrogen and natural gas is observed to be similar: τ decreases as p_i increases across the entire temperature range. In addition, the results show that the misfire limit of hydrogen and natural-gas shifts to a higher temperature range with decreasing p_i. For hydrogen jets, the results of τ can be seen to be scattered with changing p_i and T_i. These scattered results are unclear at present and need to be clarified by further experiment and calculation. However, the ignition trend for hydrogen jets can be distinguished in this graph. For natural-gas jets, ignition delay is observed to be stable with variation in p_i and T_i. At $p_i=5$ MPa, with a high chemical reaction rate, τ is much shorter than other p_i conditions. In addition, natural-gas jets can be ignited at a low T_i temperature of=860 K, and a suitably short τ for use in compression-ignition engine may be obtained at $T_i=1000$ K. This result indicates that the ignition of natural gas is strongly dependent on chemical reaction rate with changing p_i and T_i.

Figure 10 shows a comparison of heat-release rate curves for different p_i at $T_i=900$, 1000, and 1200 K. Relationships of mixture formations, chemical reaction, and τ for hydrogen and natural gas are described via the following combustion processes. At $T_i=1200$ K, similar combustion processes can be easily observed for both hydrogen and natural-gas jets. All gaseous fuel jets autoignited during injection, and a lower p_i gave a higher level of dq/dt in premixed and diffusive combustion. The increase in the dq/dt level can be explained by the good mixing and fuel accumulated because of the long delay period of lower p_i. On the other hand, with high p_i, which relates to fast mixing and high chemical reaction rate, all gaseous fuel jets spontaneously ignited just after injection and, therefore, shortened the ignition. At a lower $T_i=900$ K, dq/dt curves change slightly with hydrogen jet but alter drastically with natural gas. Lower T_i results in higher dq/dt in premixed combustion owing to long ignition delay.

Ambient pressure $p_i=2$ MPa was created to simulate premixed-charge compression-ignition (PCCI) conditions. In direct-ignition compression-ignition engines for liquid sprays, the Arrhenius τ curve at this p_i normally indicates the effect of cool flame and negative temperature coefficient (NTC) under temperature variation. In this experiment for direct-ignition compression-ignition gaseous jets, this phenomenon does not appear for both results of hydrogen and natural-gas jets. The combustion processes at this condition correspond to a higher p_i. At low ambient pressure $p_i=2$ MPa, the injection gas dilutes easily, leading to a wide mixture region in the combustion chamber. However, a low chemical reaction rate results in a reduction in the ignitability of the fuels. Owing to long ignition delay, good mixing, and accumulation of injected gas, the heat-release rate increases fast and the combustion processes produce rapid dq/dt in premixed combustion.

4.5 Effects of Varying Oxygen Concentration. In a recent engine application, an exhaust-gas recirculation (EGR) system was implemented for reducing NO_x emissions. EGR operates by recirculating a portion of an engine's exhaust-gas emissions back to the engine cylinders. To simulate EGR combustion conditions

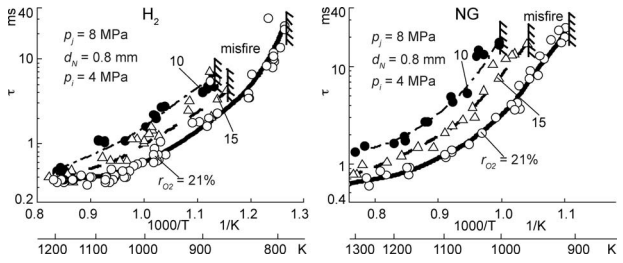

Fig. 11 Effects of r_{O2} on τ for H_2 and NG jets

in a constant-volume combustion chamber, the oxygen concentration in the ambient gas was varied from 21% to 10% by adjusting the mixing component of premixed gas.

Figures 11 and 12 show the effects of r_{O2} on τ and dq/dt for hydrogen and natural gas. In general, hydrogen and natural-gas jets exhibit similar ignition-delay trends when r_{O2} and T_i are varied. According to Fig. 11, τ increases when r_{O2} decreases across the entire temperature range. In addition, r_{O2} is observed with higher misfire temperature.

More specifically, for a hydrogen jet, different r_{O2} values do not greatly affect ignitability at high T_i of around 1200 K. In this condition, the difference in the reaction rate among r_{O2} values is small. The results of τ and dq/dt are comparable. A high ambient temperature of 1200 K corresponds to warm-up and high-load operation in real engine applications. This result suggests that the application of an EGR system for a hydrogen engine may not be suitable for reducing NO_x emissions at high T_i or high-load operation conditions. At lower T_i, the difference τ between different values of r_{O2} can be easily distinguished in Fig. 11 because of the reduction in the reaction rate. The reduction in the reaction rate can be observed via the lower initial and level heat-release rate during injection at T_i=1000 and 900 K in Fig. 12. In addition, after the injection, the reaction became extremely slow, and combustion with a very low dq/dt trailed for a long time because of the deterioration of turbulent mixing.

For natural-gas jets, variation in r_{O2} greatly affects the ignition characteristics. Ignition delay drastically increases as r_{O2} decreases, owing to a reduced reaction rate. At T_i=1200 K, the initial slope and level of dq/dt decrease drastically as r_{O2} decreases from 21% to 10%. At 1000 K, the increased fuel-air mixture together with long ignition causes a rapid release of heat in the initial combustion phase for r_{O2}=21 and 15%. However, the combustion is suppressed owing to a lack of oxygen in the reaction as r_{O2}=10%. At a lower T_i of 950 K, the low r_{O2} of 10% results in misfire, while the reaction rate for other values of r_{O2} decreases significantly, resulting in a very low dq/dt.

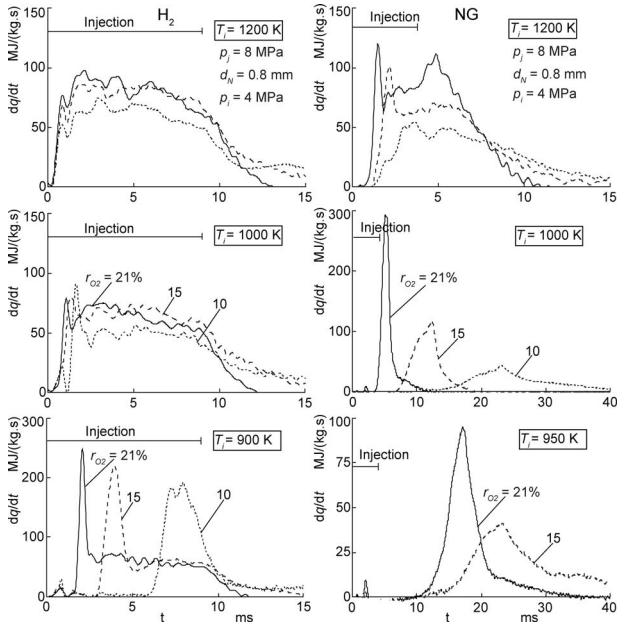

Fig. 12 Effects of r_{O2} on dq/dt for H_2 and NG jets

5 Conclusion

The fundamental ignition delay and combustion characteristics of hydrogen, natural gas, and methane jets were studied under direct-injection diesel-engine conditions. All experiments were carried out in a constant-volume vessel with variable ambient temperature, injection, and ambient conditions over a wide range. The obtained results can be summarized as follows.

1. Ambient temperature greatly affects ignition delay and heat-release rate for gaseous fuel jets, particularly at a lower temperature with a longer ignition delay.
2. Hydrogen exhibits shorter ignition delay compared with natural gas and methane over the entire temperature range. The combustion processes of these fuels correspond to some extent with the variation in temperature.
3. Stable ignition is possibly achieved during injection. A reasonably short ignition delay appropriate for compression-ignition engines can be obtained at temperatures greater than 900 K for hydrogen and 1100 K for natural gas.
4. Differing nozzle-hole diameters and injection pressures have a large effect on the ignition delay of hydrogen jets but have only a minor influence on the ignitability of a natural-gas jet.
5. The ignition delay of hydrogen and natural gas strongly depends on ambient pressure. Ignition delay drastically increases as ambient pressure decreases.
6. Low oxygen concentration leads to a longer ignition delay and a lower heat-release rate. The effect of oxygen concentration on the combustion process with changing initial slope and decreasing level heat-release rate in premixed combustion can be observed.
7. For hydrogen jets, the effects of injection and ambient conditions on ignition delays and heat-release rates are clear at ambient temperatures less than 1000 K. The scatter of ignition delay at this lower temperature is caused by the fluctuation of ambient temperature and dq/dt.

In summary, the combustion characteristics of hydrogen fuel jets can be described as a short τ and fast chemical reaction rate. A suitably short τ for application to engines can be achieved at temperatures greater than 1000 K. In a high temperature range, the results of τ and dq/dt are similar irrespective of the effects of d_N, p_j, p_i, and r_{O2}. Further, stable diffusion combustion was attained with constant dq/dt curves. At lower temperature, combustion processes were observed with long τ and high dq/dt. Under this condition, the effects of injection and ambient conditions on τ and dq/dt could be observed clearly. Shorter τ could be attained by controlling the mixture formation by decreasing p_j, enlarging d_N, increasing p_i, and increasing the oxygen mole fraction.

For natural-gas jets, τ and dq/dt tendency showed a strong dependence on temperature and was responsive to the variation in injection and ambient conditions. Ignition delay and heat-release rate were very sensitive to changes in ambient conditions T_i, p_i, and r_{O2}. Ignition delay decreased with increasing T_i, p_i, and r_{O2}. On the other hand, with varying d_N and p_j, the ignition delay exhibited different trends at high and low temperatures. At temperatures over 1000 K, the combustion characteristics of natural-gas jets were characterized with short τ and fast chemical reaction rates. Short τ were obtained with smaller d_N and p_j. However, at T_i less than 1000 K, this trend differed with short τ for larger d_N and p_j.

Acknowledgment

The authors would like to thank Mr. Tsuyoshi Morishima and Mr. Akihito Fujita for their valuable time in the experimental work.

Nomenclature

CH_4 = methane
d_N = nozzle-hole diameter, mm
dq/dt = heat-release rate, MJ/kg s
ϕ = equivalence ratio
H_2 = hydrogen
NG = natural gas
p = pressure, MPa
p_a = initial ambient pressure, MPa
p_i = ambient pressure, MPa
p_j = injection pressure, MPa
r_{O2} = oxygen concentration, %
τ = ignition delay
T_i = ambient temperature, K

References

[1] Erren, R. A., and Campbell, W. H., 1933, "Hydrogen: A Commercial Fuel for Internal Combustion Engines and Other Purposes," J. Inst. Fuel, **4**, pp. 277–291.
[2] De Boer, P. C. T., McLean, W. J., and Homan, H. S., 1976, "Performance and Emissions of Hydrogen Fueled Internal Combustion Engines," Int. J. Hydrogen Energy, **1**(2), pp. 153–172.
[3] France, D. H., 1980, "Combustion Characteristics of Hydrogen," Int. J. Hydrogen Energy, **5**(4), pp. 369–374.
[4] Ikegami, M., Miwa, K., and Shioji, M., 1982, "A Study of Hydrogen Fuelled Compression Ignition Engines," Int. J. Hydrogen Energy, **7**(4), pp. 341–353.
[5] Wong, J. K. S., 1990, "Compression Ignition of Hydrogen in a Direct Injection Diesel Engine Modified to Operate as a Low-Heat-Rejection Engine," Int. J. Hydrogen Energy, **15**(7), pp. 507–514.
[6] Lee, S. J., Yi, H. S., and Kim, E. S., 1995, "Combustion Characteristics of Intake Port Injection Type Hydrogen Fueled Engine," Int. J. Hydrogen Energy, **20**(4), pp. 317–322.
[7] Yi, H. S., Lee, S. J., and Kim, E. S., 1996, "Performance Evaluation and Emission Characteristics of in-Cylinder Injection Type Hydrogen Fueled Engine," Int. J. Hydrogen Energy, **21**(7), pp. 617–624.
[8] Seirens, R., and Resseel, E., 1998, "Backfire Mechanism in a Carburetted Hydrogen Fuelled Compression Ignition Engine," *Proceedings of the 12th World Hydrogen Conference*, Vol. 2, pp. 1537–1546.
[9] Verhelst, S., and Sierens, R., 2001, "Hydrogen Engine-Specific Properties," Int. J. Hydrogen Energy, **26**(9), pp. 987–990.
[10] Das, L. M., 1991, "Exhaust Emission Characterization of Hydrogen-Operated Engine System: Nature of Pollutants and Their Control Techniques," Int. J. Hydrogen Energy, **16**(11), pp. 765–775.
[11] Shioji, M., and Inoue, N., 1998, "Performance and NO_x Formation in a Hydrogen Premixed-Charge Engine ," *Proceedings of the 12th World Hydrogen Energy Conference*, Vol. 2, pp. 1469–1478.
[12] Karim, G. A., 2003, "Hydrogen as a Spark Ignition Engine Fuel," Int. J. Hydrogen Energy, **28**(5), pp. 569–577.
[13] Shioji, M., and Ishiyama, T., 2002, "Feasibility of the High Speed Hydrogen Engine," International Symposium on Hydrogen Engine, pp. 1–9.
[14] Tang, X., Natkin, R. L., Boyer, B. A., Oltmans, B. A., and Potts, C., 2003, "Hydrogen IC Engine Boosting Performance and NO_x Study," SAE Paper No. 2003-01-0631.
[15] Knecht, W., Hakimifard, D., and Carletta, M., 1984, "A Hydrogen Engine for Heavy Duty Vehicles," SAE Paper No. 845138.
[16] Saravanan, N., and Nagarajan, G., 2008, "An Experimental Investigation of Hydrogen-Enriched Air Induction in a Diesel Engine System," Int. J. Hydrogen Energy, **33**(6), pp. 1769–1775.
[17] Kondo, T., Himura, M., and Furuhama, S., 1996, "A Study on the Mechanism of Backfire in External Mixture Formation Hydrogen Engines," *Proceedings of the 11th World Hydrogen Energy Conference*, Vol. 2, pp. 1547–1556.
[18] Shioji, M., Eguchi, S., Kitazaki, M., and Mohammadi, A., 2004, "Knock Characteristics and Performance in an SI Engine With Hydrogen and Natural-Gas Blended Fuels," SAE Paper No. 2004-01-1929.
[19] Mohammadi, A., Shioji, M., Nakai, Y., Ishikura, W., and Tabo, E., 2007, "Performance and Combustion Characteristics of a Direct Injection SI Hydrogen Engine," Int. J. Hydrogen Energy, **32**(2), pp. 296–304.
[20] Ishiyama, T., Shioji, M., Ihara, T., and Inoue, N., 2003, "Characteristics of Spontaneous Ignition and Combustion in Unsteady High-Speed Gaseous Fuel Jets," SAE Paper No. 2003-01-1922.
[21] Mohammadi, A., Shioji, M., Matsui, Y., and Kajiwara, R., 2008, "Spark-Ignition and Combustion Characteristics of High-Pressure Hydrogen and Natural-Gas Intermittent Jets," ASME J. Eng. Gas Turbines Power, **130**(6), p. 062801.
[22] Ristovski, Z. D., Morawska, L., Ayoko, G. A., Johnson, G., Gilbert, D., and Greenaway, C., 2000, "Particulate Emissions From a Petrol to CNG Converted Spark Ignition Vehicle," J. Aerosol Sci., **31**, pp. 624–625.
[23] Ristovski, Z. D., Morawska, L., Hitchins, J., Thomas, S., Greenaway, C., and Gilbert, D., 2000, "Particle Emissions From Compressed Natural Gas Engines," J. Aerosol Sci., **31**(4), pp. 403–413.
[24] Selim, M. Y., Radwan, M., and Saleh, H., 2008, "Improving the Performance of Dual Fuel Engines Running on Natural Gas/LPG by Using Pilot Fuel Derived From Jojoba Seeds," Renewable Energy, **33**(6), pp. 1173–1185.
[25] Akansu, S. O., Dulger, Z., Kahraman, N., and Veziroglu, T. N., 2004, "Internal Combustion Engines Fueled by Natural Gas-Hydrogen Mixtures," Int. J. Hydrogen Energy, **29**(14), pp. 1527–1539.
[26] Gambino, M., Iannaccone, S., and Unich, A., 1991, "Heavy-Duty Spark Ignition Engines Fueled With Methane," ASME J. Eng. Gas Turbines Power, **113**(3), pp. 359.
[27] Willi, M. L., and Richards, B. G., 1995, "Design and Development of a Direct Injected, Glow Plug Ignition-Assisted, Natural Gas Engine," ASME J. Eng. Gas Turbines Power, **117**(4), pp. 799–803.
[28] Saravanan, N., Nagarajan, G., and Narayanasamy, S., 2008, "An Experimental Investigation on DI Diesel Engine With Hydrogen Fuel," Renewable Energy, **33**(3), pp. 415–421.
[29] Yap, D., Peucheret, S., Megaritis, A., Wyszynski, M., and Xu, H., 2006, "Natural Gas HCCI Engine Operation With Exhaust Gas Fuel Reforming," Int. J. Hydrogen Energy, **31**(5), pp. 587–595.
[30] Naber, J. D., and Siebers, D. L., 1998, "Hydrogen Combustion Under Diesel Engine Conditions," Int. J. Hydrogen Energy, **23**(5), pp. 363–371.
[31] Naber, J. D., Siebers, D. L., Di Julio, S. S., and Westbrook, C. K., 1994, "Effects of Natural Gas Composition on Ignition Delay Under Diesel Conditions," Combust. Flame, **99**(2), pp. 192–200.